Effective conductivity of inertial flows through porous media

Gerardo SEVERINO[1], Francesco GIANNINO[2], Francesco DE PAOLA[3] and Vittorio DI FEDERICO[4]

[1]*Division of Water Resources Management*, University of Naples - FEDERICO II
via Universitá 100 - I80055, Portici (NA), ITALY (e-mail: gerardo.severino@unina.it)

[2]*Division of Ecology and System Dynamics*, University of Naples - FEDERICO II
via Universitá 100 - I80055, Portici (NA), ITALY (e-mail: francesco.giannino@unina.it)

[3]*Division of Hydraulics*, University of Naples - FEDERICO II
via Claudio 21 - I80125, Napoli (NA), ITALY (e-mail: francesco.depaola@unina.it)

[4]*Department of Civil, Chemical, Environmental, and Materials Engineering*, University of Bologna - ALMA MATER STUDIORUM
viale Risorgimento 2 - I40136, Bologna (BO), ITALY (e-mail: vittorio.difederico@unibo.it)

We study two-dimensional incompressible inertial flows through porous media. At core (small) scale, we prove that the constitutive, nonlinear model can be re-written into a linear one by means of a new parameter $K^\star$ which encompasses all the inertial effects. In natural (large scale) formations, $K^\star$ is erratically changing, and we compute analytically its counterpart, which is coined *generalized effective conductivity* (GEC), by the *self-consistent approach* (SCA). In spite of its approximate nature, the SCA leads to simple results that are in good agreement with *Monte Carlo simulations* (MCs).

INTRODUCTION

High velocity flows through porous formations are encountered in several industrial and environmental applications, such as flow in chemical reactors, extraction of oil and gas from reservoirs, flow through rock-fill dams or in the zones surrounding pumping/injecting wells.

The adopted (constitutive) model is usually the Darcy's law, i.e. $K\boldsymbol{J} = \boldsymbol{v}$, relating the velocity field $\boldsymbol{v}$ to the gradient $\boldsymbol{J} \equiv -\nabla h$ of the head h via the conductivity K [1]. However, when the magnitude $J \equiv |\boldsymbol{J}|$ increases, so does the velocity, and concurrently the Darcy's model is not adequate, anymore. In this case, the pertinent flow regime is the Forchheimer's one, which accounts also for the impact of the inertial terms, besides the viscous ones [2]. Within the constitutive model, these effects are modelled by an extra term proportional to the magnitude $|\boldsymbol{v}| = \sqrt{\boldsymbol{v} \cdot \boldsymbol{v}}$ of the velocity, i.e.

$$K\boldsymbol{J} = \left(1 + \beta\sqrt{K}|\boldsymbol{v}|\right)\boldsymbol{v}, \tag{1}$$

where $\beta > 0$ quantifies the impact of the inertial terms [e.g. 3]. In particular, for $\beta \to 0$ eq. (1) reduces to the Darcy's law. Alternative formulations, based on the concept of energy-dissipation, have been also proposed [see 4, and references therein].

The Forchheimer's model (1) applies only to homogeneous media, and concurrently it is not suitable for natural geologic formations, where both K and β vary in the space over several orders of magnitude [5, 6]. These erratic fluctuations have a decisive impact upon flow evolving in geological formations [see, e.g. 7]. Generally, such variations are modelled within a stochastic framework that regards K and β as random fields [a comprehensive exposition can be found in 8]. As a matter of fact, the flow variables become stochastic.

One of the aim in the theory of flows through heterogeneous media pertains to the derivation of a constitutive model satisfied by the average variables. The coefficient that relates the mean velocity $\langle\boldsymbol{v}\rangle$ to the mean gradient $\langle\boldsymbol{J}\rangle$ is termed "effective conductivity". Computing this latter has a long tradition traced back to [9], and subsequently forwarded to numerous branches of Physics such as electricity, wave scattering and the theory of elasticity [for a wide review, see 10, 11, and references therein]. In porous media fluid mechanics, the same problem has been pioneered by [8] in the case of mean uniform Darcy-type flows. More recently, such an approach has been extended to non uniform mean (such as source-type) flows by [12]. Likewise, the natural question is whether one can derive an effective conductivity also for flows in the Forchheimer's regime. This problem has received a scarse attention [with the exceptions of the studies of 7, 13, 14], its importance notwithstanding.

In the present study we investigate how the spatial variability of the β-coefficient and the conductivity K affects the GEC. The latter is computed by means of the SCA, which regards the formation as a bundle of inclusions set at random in the space. Then, the GEC is derived by requiring that it is equal to the conductivity of the medium as a whole [15].

The paper is organized as follows. We first cast the Forchheimer's model in a form which enables one to treat it like the Darcy's law. Subsequently, we derive the expression of the GEC, and discuss its general properties. Then, we move to the discussion of results after adopting a (fairly general) model for the bivariate distribution of the random pair (K, β). We end up with concluding remarks, with a few highlights on potential applicability of our results.

GENERAL RESULTS

We consider steady flow driven by a gradient $\boldsymbol{J} \equiv (J_x, J_y)$ in a two-dimensional, unbounded domain. The flow obeys the Forchheimer's law (1). In order to cast the latter in the form of a Darcy-type model, we rewrite eq. (1) in terms of its scalar

components:

$$K = \left(1 + \beta \, |\boldsymbol{J}| \, \sqrt{K} \left|\frac{v_\gamma}{J_\gamma}\right|\right) \frac{v_\gamma}{J_\gamma}, \quad (\gamma = x, y), \qquad (2)$$

with $|\boldsymbol{J}| \equiv J = \left(J_x^2 + J_y^2\right)^{1/2}$. Hence, solving eq. (2) with respect to the unknown v_γ/J_γ, and back substitution into eq. (1), leads to a Darcy's type constitutive model, i.e. $K^\star \boldsymbol{J} = \boldsymbol{v}$, where now the conductivity $K^\star$ is given by:

$$K^\star \equiv K^\star(K,\beta) = \frac{2K}{1 + \sqrt{1 + 4J\beta K^{3/2}}}. \qquad (3)$$

It is important to underline that such a procedure does not destroy the non-linearity (i.e. inertial effects) of the flow problem, being the original non-linearity now encapsulated into the new conductivity (3). The importance of casting the Forchheimer's law (1) within a model resembling *de facto* the Darcy's one, is that, in accordance with the continuum mechanics approach [1], one can use the former for all applications relying upon the Darcy's model, by replacing $K \to K^\star$, solely. A similar result, which can be achieved also by dealing with the Forchheimer model (1) written in norm, has been obtained by [13]. In particular, for $\beta \to 0$ one recovers the classical Darcy's law. On the other hand, a very large value of β is attached to a flow dominated by inertia, and concurrently the velocity drastically decreases (ultimately vanishing for $\beta \to \infty$).

To quantify the importance of the Forchheimer's conductivity (3) relative to the Darcy's one, FIGURE 1 depicts the ratio $K^\star/K$ as function of $J\beta K^{3/2}$. The latter parameter quantifies the importance of the inertial terms relative to the viscous ones, and therefore can be considered akin to a Reynolds number [see, e.g. 16]. It is seen that the occurrence of one of the two (i.e. Forchheimer *vs* Darcy) regimes depends upon a dimensionless combination of: i) the inertial coefficient β, ii) the power $K^{3/2}$, and iii) the magnitude of the gradient J. As a consequence, even for highly inertial flows (large β) one can still deal with a Darcy (purely viscous) flow, provided that a very poorly conducting medium, with a small gradient, is considered. In particular, inspection from FIGURE 1 suggests that the Darcy's regime applies whenever $J\beta K^{3/2} < 10^{-1}$. Conversely, the Forchheimer's regime becomes predominant for $J\beta K^{3/2} > 10^2$. The range $10^{-1} < J\beta K^{3/2} < 10^2$ covers the transition from one regime to the other. The occurrence of three different flow regimes, in dependence of the Reynolds number $J\beta K^{3/2}$, was also pointed out by [17] and [18]. With these prerequisites, we are now in position to compute the generalized effective conductivity $\mathrm{K}^{\mathrm{eff}}$ by means of the SCA.

Generalized effective conductivity (GEC)

Due to the natural heterogeneity of porous formations, regarding the pair (K, β) as constant is too simplistic. In fact, they usually, with K in particular, vary in the space in a manner which does not allow modelling them by a deterministic approach. For this reason, it is customary to regard the pair (K, β) as Gaussian, bivariate, stationary, random field [19]. As a consequence, the flow variables become
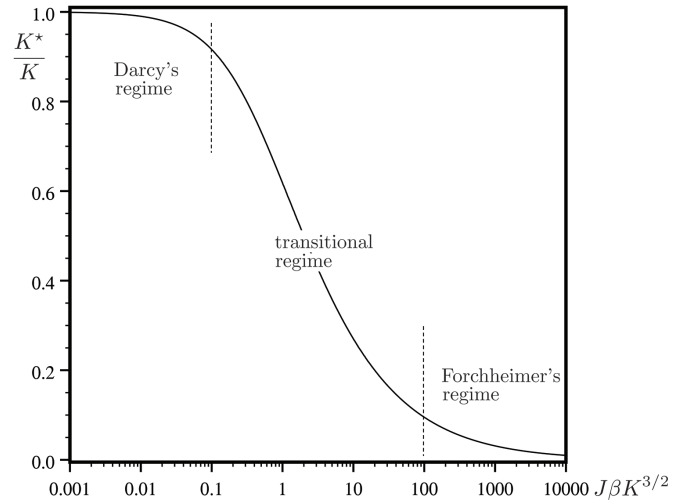

FIG. 1. Dependence of the ratio between the Forchheimer conductivity $K^\star$ relative to the Darcy's one K versus the non dimensional group $J\beta K^{3/2}$ of the flow's parameters.

stochastic, and we are interested here into quantifying their mean values. In particular, we aim at computing the coefficient $\mathrm{K}^{\mathrm{eff}}$ (known as *effective conductivity*) relating the mean velocity $\langle \boldsymbol{v} \rangle$ to the mean gradient $\langle \boldsymbol{J} \rangle$, i.e. $\mathrm{K}^{\mathrm{eff}} \langle \boldsymbol{J} \rangle = \langle \boldsymbol{v} \rangle$. This effective constitutive model, together with the mass conservation $\nabla \cdot \langle \boldsymbol{v} \rangle = 0$, can be used to solve various problems of practical interest. In other words, inertial flows through heterogeneous porous media are tackled by considering a homogeneous (fictitious) medium of effective conductivity. While this topic is well established for flows in the Darcyan regime [see, e.g. 20], to our knowledge, there are a very few studies [13, 14] dealing with the analogous problem in the Forchheimer's regime.

Here, the effective conductivity is computed by means of the SCA [21]. Thus, the formation is regarded as a bundle of many, randomly arranged, non overlapping, circular inclusions embedded into a matrix (background) of constant conductivity K_∞ (FIGURE 2-a)). Each inclusion has a $K^\star$-value which is now random in the space. Then, by invoking ergodicity, the above single realization is replaced by the ensemble average, and concurrently interaction among inclusions becomes that of a single inclusion implanted into a medium which is homogenized by means of the effective conductivity $\mathrm{K}^{\mathrm{eff}}$ (FIGURE 2-b)). It is therefore clear that the core of the SCA is how a uniform flow field is "deformed" by a circular inclusion $\Omega^\star$ of conductivity $K^\star$ different from the conductivity K_∞ of the background Ω_∞. This approach has been implemented in numerous branches of Physics, such as Electromagnetism, Heat Transfer and Diffusion [see, e.g. 15], and therefore, although results in the present study pertain to random porous media, they nevertheless find application in a much wider spectrum, where nonlinear constitutive laws are concerned.

In order to grasp the effect of the inertia for the problem at stake, it suffices dealing with the flow-net as distorted by a single inclusion (of radius R), being the effective conductivity
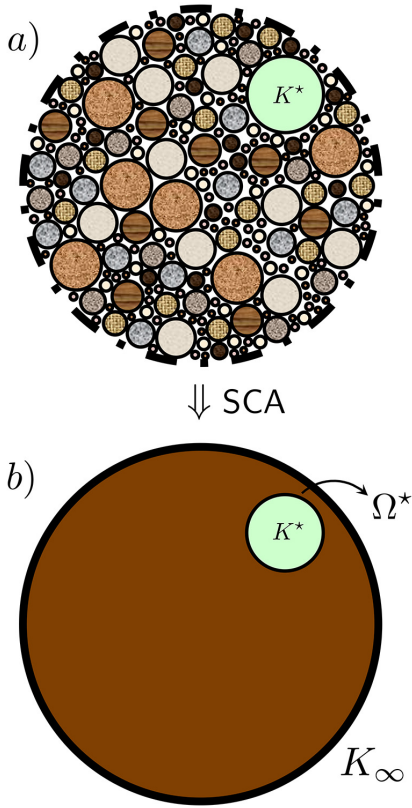
FIG. 2. *a*) Sketch of the heterogeneous (circular with a large radius) medium made up of many circular inclusions of randomly distributed conductivities, and *b*) its transition to an effective medium by means of the SCA.

computed as ensemble average over many of such single realizations. For this reason, in FIGURE 3 we depict the contour levels of the scaled head (red dashed lines):

$$\frac{h}{R} = \kappa^\star \frac{x}{R} \begin{cases} 1 + \dfrac{(1-\kappa^\star)/(1+\kappa^\star)}{(x/R)^2 + (y/R)^2} & (x,y) \in \Omega_\infty \\[4mm] \dfrac{2}{1+\kappa^\star} & (x,y) \in \Omega^\star, \end{cases} \tag{4}$$

and the stream function (blue continuous lines):

$$\frac{\Psi}{RK_\infty} = \frac{y}{R} \begin{cases} 1 - \dfrac{(1-\kappa^\star)/(1+\kappa^\star)}{(x/R)^2 + (y/R)^2} & (x,y) \in \Omega_\infty \\[4mm] \dfrac{2\kappa^\star}{1+\kappa^\star} & (x,y) \in \Omega^\star, \end{cases} \tag{5}$$

pertaining to a Forchheimer-type flow (uniform at infinity), and disturbed by an inclusion, being

$$\kappa^\star \equiv \frac{K^\star}{K_\infty} = 2\frac{K}{K_\infty}\left(1 + \sqrt{1 + 4J\beta K^{3/2}}\right)^{-1}. \tag{6}$$

The contrast ratio $\kappa^\star$ quantifies the impact of $K^\star$ relative to that of the background K_∞. For illustration purposes,
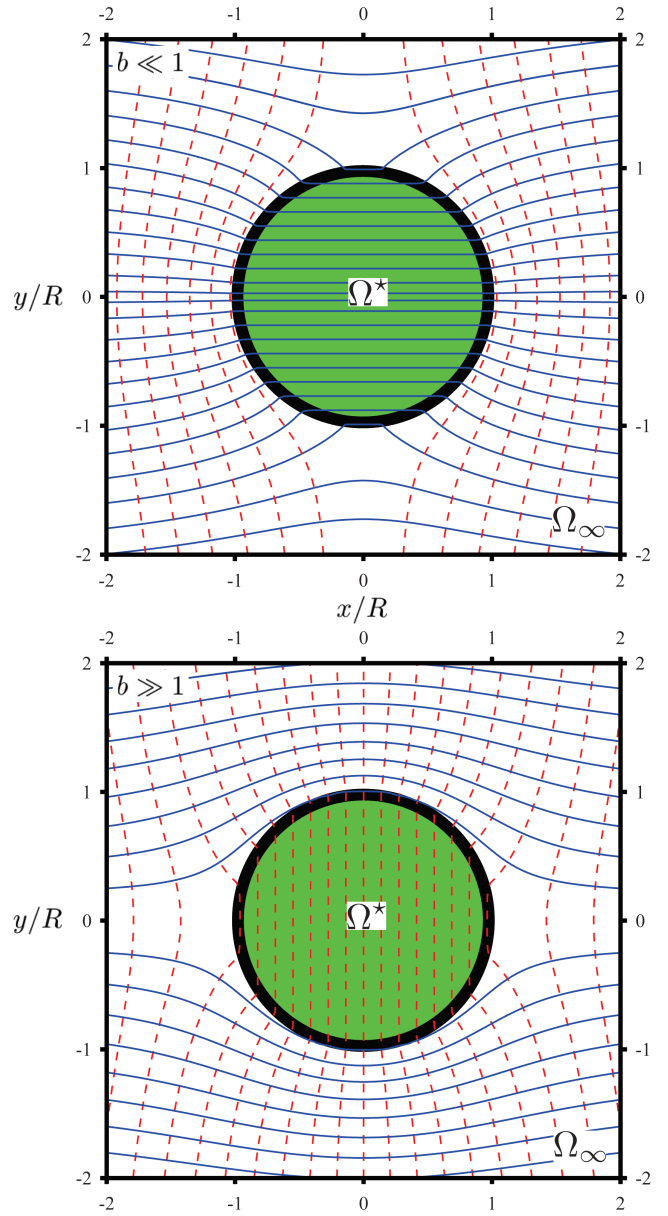

FIG. 3. Contour-plot of the scaled head eq. (4) and stream function eq. (5) for given ratio $K/K_\infty = 10/1$ and two, widely different, values of $b \equiv J\beta K^{3/2}$ referring: i) to the Darcy's, i.e. $b \ll 1$, and ii) to the Forchheimer's regime, i.e. $b \gg 1$, respectively. Lengths are scaled by the radius R of the circular inclusion (whose center is set at the origin of the framework).

in FIGURE 3 the ratio K/K_∞ is taken equal to 10/1. Hence, for $b \equiv J\beta K^{3/2} \ll 1$ the flow lies within the Darcy's regime (see FIGURE 1), and the inclusion $\Omega^\star$ acts like an attractor for the stream lines (upper picture in FIGURE 3), since in this case one has $\kappa^\star \simeq K/K_\infty = 10$ [see, e.g. 22]. Conversely, when $b \equiv J\beta K^{3/2} \gg 1$ (a circumstance calling for the Forchheimer's regime) $K^\star$ becomes so small that $\Omega^\star$ now behaves like a flow barrier (lower picture in FIGURE 3).

To compute the GEC by means of the SCA, one has first to derive the ensemble averages of: i) the velocity $\langle \boldsymbol{v} \rangle$, and ii)

the head-gradient $\mathbf{E} \equiv -\nabla \langle h \rangle$. Subsequently, the GEC is obtained by requiring that it fits the equation $\langle v \rangle - \mathbf{K}^{\text{eff}} \mathbf{E} = 0$. It is therefore clear that the crux of the matter consists into calculating the expression of the local velocity v as well as of the gradient J, as function of $K^\star \equiv K^\star(Y, \zeta)$ and of the given (i.e. constant) head-gradient $\langle J \rangle$ applied at the boundary of the flow domain. These two quantities were computed by [23], and we quote here only the final result, i.e.

$$J = -\left(1 + \frac{K_\infty - K^\star}{K_\infty + K^\star}\right) \langle J \rangle, \quad v = -\frac{2 K_\infty K^\star}{K_\infty + K^\star} \langle J \rangle, \quad (7)$$

with the conductivity $K^\star$ given by (3). Thus, by taking the ensemble averages of (7), it yields:

$$\mathbf{E} = -\left[1 + \int \mathrm{d}K \, \mathrm{d}\beta \, f(K, \beta) \frac{K_\infty - K^\star}{K_\infty + K^\star}\right] \langle J \rangle, \quad (8)$$

$$\langle v \rangle = -2 K_\infty \left[\int \mathrm{d}K \, \mathrm{d}\beta \, \frac{f(K, \beta) K^\star}{K_\infty + K^\star}\right] \langle J \rangle, \quad (9)$$

being $f \equiv f(K, \beta)$ the bivariate probability density function. The difference with previous results [see, e.g. 22] stems from the dependence of the conductivity also upon the inertial parameter β. Then, application of the above stated definition of effective conductivity (with $K_\infty \equiv \mathbf{K}^{\text{eff}}$) leads to:

$$1 + \int \mathrm{d}K \, \mathrm{d}\beta \, f(K, \beta) \frac{\mathbf{K}^{\text{eff}} - K^\star}{\mathbf{K}^{\text{eff}} + K^\star} - 2 \int \mathrm{d}K \, \mathrm{d}\beta \, \frac{f(K, \beta) K^\star}{\mathbf{K}^{\text{eff}} + K^\star} = 0. \quad (10)$$

This equation can be rearranged, after some algebraic manipulations relaying upon the property $\int \mathrm{d}K \mathrm{d}\beta \, f(K, \beta) = 1$, as:

$$\int \mathrm{d}K \, \mathrm{d}\beta \, f(K, \beta) \frac{K^\star - \mathbf{K}^{\text{eff}}}{K^\star + \mathbf{K}^{\text{eff}}} = 0. \quad (11)$$

The equation (11) generalizes eq. (3.4.45) in [8]; in fact, for $\beta \to 0$ it yields $K^\star \to K$, and one recovers the governing equation for the effective conductivity in the Darcy's regime. Like the effective Darcy's law [see, e.g. 24], even the GEC results a local medium's property (locality), whose scalar nature is due to the isotropic heterogeneity's structure of K and β [see the exhaustive review on the matter in 6, 14].

We wish to establish upper/lower bounds for the GEC. Toward this aim, we note that the continuous function:

$$\mathscr{F}(t) = \int \mathrm{d}K \, \mathrm{d}\beta \, f(K, \beta) \frac{K^\star - t}{K^\star + t} \quad (12)$$

is monotonously decreasing with $\mathscr{F}(0) = 1$, and $\mathscr{F}(\infty) = -1$, and therefore $\mathbf{K}^{\text{eff}}$ is determined uniquely (black line in FIGURE 4) by computing (numerically) the root of (12). Moreover, since $\mathscr{F} \equiv \mathscr{F}(t)$ is a convex function, one can get a lower bound $\mathbf{K}^{\text{eff}}_<$ for the GEC by dealing with the zero, i.e. $\mathbf{K}^{\text{eff}}_< = -1/\mathscr{F}'(0)$, of the tangent (red line in the insert of FIGURE 4) to the function $\mathscr{F}(t)$ at $t = 0$. Hence, upon evaluation of the derivative $\mathscr{F}'(t)|_{t=0}$, it yields:

$$\mathbf{K}^{\text{eff}}_< = \frac{1}{2} \left[\int \mathrm{d}K \, \mathrm{d}\beta \, \frac{f(K, \beta)}{K^\star}\right]^{-1} = \frac{1}{2} \left\langle \frac{1}{K^\star} \right\rangle^{-1} = \frac{K^\star_H}{2}. \quad (13)$$
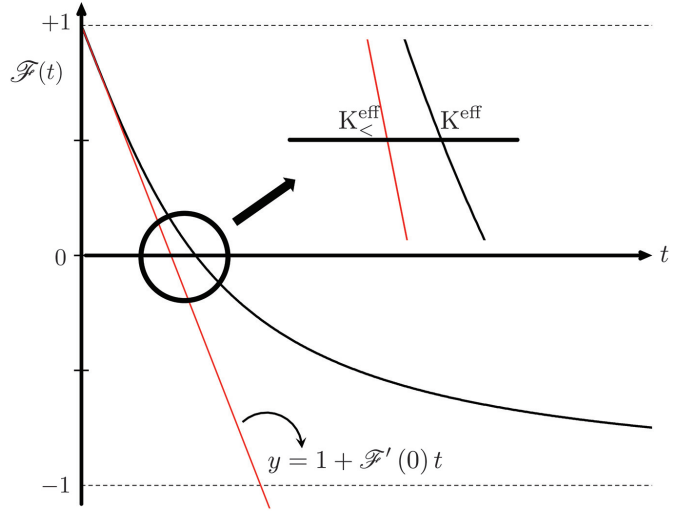

FIG. 4. Sketch illustrating the method to get a lower bound $\mathbf{K}^{\text{eff}}_<$ of the GEC, by dealing with the root of the tangent (red line) to the function $\mathscr{F}(t)$ at $t = 0$.

Thus, one can claim that the half of the harmonic mean $K^\star_H$ represents a lower bound for the GEC. The upper bound $\mathbf{K}^{\text{eff}}_>$ is obtained by applying the same reasoning as before with t in (12) replaced by $1/t$. The final result is:

$$\mathbf{K}^{\text{eff}}_> = 2 \int \mathrm{d}K \, \mathrm{d}\beta \, f(K, \beta) K^\star = 2 K^\star_A, \quad (14)$$

being $K^\star_A$ the arithmetic mean. To summarize, the GEC lies within the interval $[K^\star_H/2, 2K^\star_A]$, which is slightly larger than that, i.e. $[K_H, K_A]$, pertaining to a purely Darcy's flow. This is due to the fact that, unlike the Darcy's regime (where the effective conductivity is affected by the uncertainty of a single quantity), here the extra stochastic nature of the parameter β de facto enlarges the range of variability of $\mathbf{K}^{\text{eff}}$. A similar conclusion, although by a different approach, was achieved by [14]. Other bounds can be obtained by employing the variational approach, in close analogy to [25], or by means of the energy-dissipation concept [8].

The above general results provide direct means to grasp the main features of the mean velocity field, when a small amount of information about the statistics of the pair (K, β) is available. Noteworthy, they are also useful for codes providing the numerical solution of eq. (11). In what follows, we discuss the structure and the properties of the GEC for a fairly general model of bivariate joint probability density function $f \equiv f(K, \beta)$.

DISCUSSION

The non linear equation (11) allows computing the GEC, once the model for the bivariate probability distribution function $f \equiv f(K, \beta)$ is selected. While there is a large body of field data suggesting that both $\ln K$ [see the comprehensive review in 6] and $\ln \beta$ [an updated review can be found in 14, and

references therein] can be modelled as Gaussian, the cross-correlation $\ln K$–$\ln \beta$ deserves a further discussion. The most exhaustive reviews on this topic are from [26] and [27], who showed that the inertial coefficient is significantly affected by the conductivity's heterogeneity, displaying, in particular, an overall negative correlation (i.e. $\rho \leq 0$) with the conductivity K [in line with 19]. For these reasons, in what follows we shall regard $K = K_G \exp Y$ and $\beta = \beta_G \exp \zeta$ as a normally distributed, negatively correlated random variables, being K_G–β_G and Y–ζ the geometric means and the fluctuations, respectively.

FIGURE 5 shows the scaled $\text{K}^{\text{eff}}/K_G$ versus the dimensionless parameter $b_G \equiv J\beta_G K_G^{3/2} \in [10^{-4}; 10^4]$ [for a wide overview of the values taken by β_G and K_G, see 6, 28, respectively], for several values of the variances σ_Y^2 and σ_ζ^2, that are taken equal for simplicity (similar conclusions are drawn for $\sigma_Y^2 \neq \sigma_\zeta^2$). In particular, we have considered two cases: i) uncorrelated, and ii) negatively correlated Y–ζ, which cover the majority of the practical situations. The behavior at small b_G–values (Darcyan regime) can be elucidated after expanding the term $(K^\star - \text{K}^{\text{eff}})/(K^\star + \text{K}^{\text{eff}})$ appearing into eq. (11) in MacLaurin-series of b_G. Omitting the algebraic details, the governing equation for $\kappa = \text{K}^{\text{eff}}/K_G$ writes has:

$$\int_{\mathbb{R}} dY \exp\left(-\frac{Y^2}{2\sigma_Y^2}\right) \frac{\exp Y - \kappa}{\exp Y + \kappa} - b_G \Upsilon_\kappa \simeq 0, \quad (15)$$

being $\Upsilon_\kappa \equiv \Upsilon_\kappa(\rho, \sigma_Y, \sigma_\zeta)$ a non negative function (whose cumbersome expression is not relevant for the discussion at stake). As such, in the Darcyan regime the GEC results smaller than the first term on the left hand side in eq. (15), which coincides with the expression obtained by [8]. The reduction of the GEC with increasing variances is explained by noting that, in these cases, in most of the points of the flow domain the (K, β)–values differ significantly from their means, and concurrently the GEC lies still within the transitional regime (see FIGURE 1), the small b_G notwithstanding.

The most evident feature is that the GEC turns out to be a monotonously decreasing function of b_G. To provide a physical explanation, we may focus on the flow's pattern determined by a single inclusion (see FIGURE 3 with b replaced by b_G), since the GEC is computed as ensemble average over many of these realizations. Thus, as discussed above, streamlines circumvent the inclusion $\Omega^\star$ for $b_G \gg 1$. As a consequence, streamlines (and concurrently the mean flux) entering the inclusion reduce. Since the mean gradient $\langle \boldsymbol{J} \rangle$ is constant, the GEC reduces. A similar argument is the key to explain the increase of K^{eff} with negatively increasing correlation between Y and ζ. Toward this aim, it is convenient dealing with (6) that, upon substitutions $K = K_G \exp Y$ and $\beta = \beta_G \exp \zeta$, reads as:

$$\kappa^\star = 2\frac{K_G}{K_\infty} \exp Y \left[1 + \sqrt{1 + 4b_G \exp\left(\zeta + \frac{3}{2}Y\right)}\right]^{-1}. \quad (16)$$

Thus, an increase of ζ implies a (linear) reduction of Y. Since the quantity in the square brackets into (16) does not change
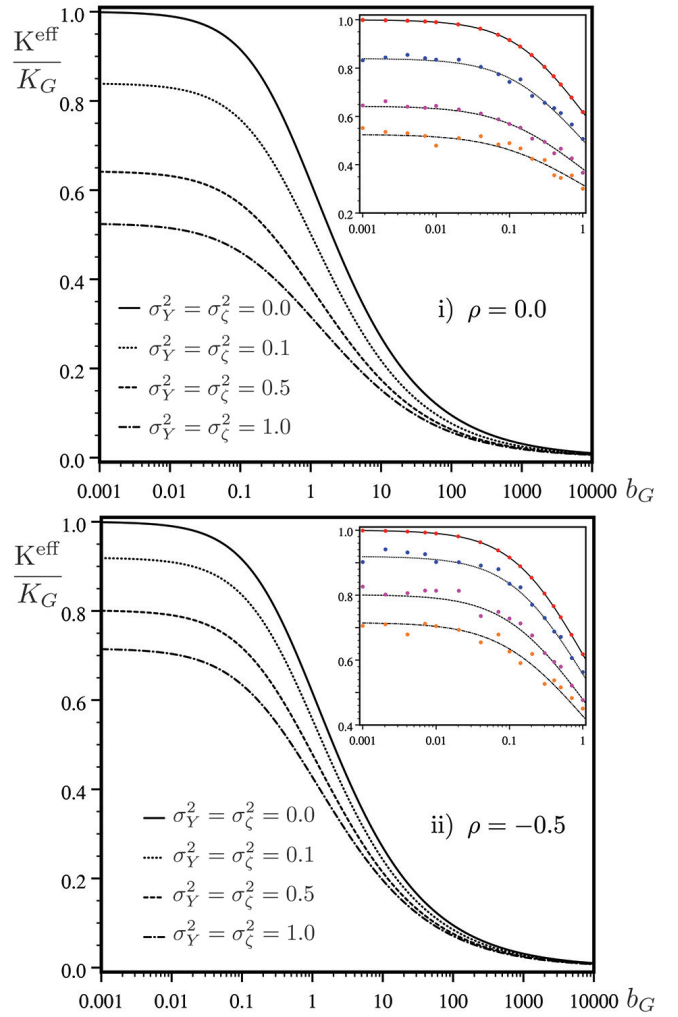

FIG. 5. Normalized GEC as function of $b_G \equiv J\beta_G K_G^{3/2}$, and given values of the variances $\sigma_Y^2 = \sigma_\zeta^2$ for: i) uncorrelated, and ii) negatively correlated Y–ζ. The inserts show a comparison between MCs (symbols) and the analytical model (lines).

significantly for any given b_G, one can claim that streamlines entering the inclusion thin out (due to the reduction of K_G/K_∞). Hence, the gradient reduces (see the lower picture in FIGURE 3), and concurrently the GEC increases in order to adjust the flux passing through the boundary $\partial\Omega^\star$ of the inclusion, as demanded by the mass conservation principle. Finally, to corroborate our analytical results, Monte Carlo simulations have been carried out, as well. For the sake of completeness, we describe herein the procedure leading to the MCs. Thus, any realization of the Gaussian, stationary, correlated, random fields Y and ζ is generated (by means of Cholesky decomposition), and subsequently mapped upon a numerical (50×50 nodes) mesh (step-i). Then, the system of flow equations

$$\begin{cases} \partial_\gamma v_\gamma = 0 \\ -K \partial_\gamma h = \left(1 + \beta\sqrt{K}\,|\boldsymbol{v}|\right) v_\gamma \end{cases}$$

is converted into a set of algebraic equations (finite difference method) which are solved (iteratively) for the nodal-values of the head and concurrently of the velocity (step-ii), to provide results for a *single realization*. The domain Ω is a square, whose center coincides with the origin $(0,0)$, where on two apart (vertical) sides the boundary condition is that of "given" head drop up/downstream, whereas along the remaining parallel (horizontal) sides a zero (vertical) velocity boundary condition is imposed. These boundary conditions are deterministic, and therefore they are the same in all the realizations. Finally, steps i)-ii) are iterated to obtain at each node results for multiple (i.e. $\mathcal{N}_r = 5000$) realizations. Hence, the GEC is evaluated at the center of Ω (since this point is sufficiently far away from the boundaries, whose impact is not accounted for in the analytical model) as follows:

$$\mathbf{K}^{\text{eff}} \simeq - \left[\sum_{i=1}^{\mathcal{N}_r} v_x^i(0,0) \right] / \left[\sum_{i=1}^{\mathcal{N}_r} \partial_x h^i(0,0) \right]. \qquad (17)$$

The numerical simulations (symbols in the inserts of FIGURE 5) are in good agreement with their analytical counterparts (continuous lines).

To conclude, we wish to emphasize that the analytical expression of the GEC relies on a quite robust, seldom encountered [see e.g. 14] assumption about the shape of the bivariate probability density function f. In addition, it is not limited to small variances of Y and ζ.

CONCLUSIONS

We have studied a two-dimensional, high velocity, steady flow through a porous medium. The constitutive (Forchheimer) model is cast in a Darcy-type equation, where the coefficient $K^\star$ is shown to coincide with the Darcy's conductivity, i.e. K, when the inertial parameter β vanishes. This enables one to treat flow in the Forchheimer regime like that occurring in the Darcy's one, simply by replacing $K \to K^\star$. Three different flow regimes are identified, and they span from a purely viscous one, till to that dominated by inertial effects. In the intermediate regime, both viscous and inertial forces influence the flow.

Besides the theoretical interest, our study provides a way of

modelling the stochastic heterogeneity of porous media. Thus, we have focused on the computation of the generalized effective conductivity (GEC) by means of the SCA. The GEC is derived by assuming that: (i) the background surrounding each inclusion is homogeneous; this approximation is reasonable when interactions between blocks can be neglected. (ii) Inclusions are circular, that is an accurate approximation for isotropic formations. (iii) The domain is large enough to allow adoption of the ergodicity assumption. Although assumptions (i)–(iii) are clearly approximations, they nevertheless do not limit the accuracy of results, as demonstrated by means of Monte Carlo simulations.

General (i.e. valid for any bivariate probability density function f) bounds for the GEC are derived. They result slightly larger than those known for the effective Darcy's conductivity, as consequence of the larger uncertainty attached to the stochastic nature of the β–parameter. The structure and the properties of the GEC are discussed for a fairly general shape of f. In particular, the GEC is found to increase for reduced values of the coefficient of correlation between the log-transforms of the conductivity and the inertial parameter, as well as of the variances of the former parameters and of the Reynolds number. This is explained straightforwardly as a consequence of the mass conservation.

Our results find application in the study of flow and transport through strongly heterogeneous (with large variances) porous formations. Noteworthy, they can also be used as benchmark to validate complex numerical codes. Finally, the present study may serve as starting point to come up with an effective Forchheimer's law, in close analogy to the approach developed for stratified formations [14, 29, 30].

ACKNOWLEDGMENTS

REFERENCES

[1] J. Bear, *Dynamics of fluids in porous media* (Courier Corporation, 2013).

[2] H. Ma and D. Ruth, Transport in Porous Media **13**, 139 (1993).

[3] M. Agnaou, D. Lasseux, and A. Ahmadi, Physical Review E **96**, 043105 (2017).

[4] F. Russo Spena and A. Vacca, Transport in Porous Media **45**, 405 (2001).

[5] U. Costa, J. Andrade Jr, H. Makse, and H. Stanley, Physica A: Statistical Mechanics and its Applications **266**, 420 (1999).

[6] Y. Rubin, *Applied Stochastic Hydrogeology* (Oxford University Press, 2003).

[7] S. Rojas and J. Koplik, Physical Review E **58**, 4776 (1998).

[8] G. Dagan, *Flow and transport in porous formations* (Springer-Verlag GmbH & Co. KG., 1989).

[9] J. M. Beran, *Statistical Continuum Theories* (Interscience, New York, 1968).

[10] G. W. Milton, *The theory of composites* (Cambridge University Press, 2002).

[11] S. Torquato, *Random heterogeneous materials: microstructure and macroscopic properties* (Springer Science & Business Media, 2013).

[12] G. Severino, F. De Paola, and G. Toraldo, Phys. Rev. Fluids **7**, 064101 (2022).

[13] J.-L. Auriault, C. Geindreau, and L. Orgéas, Transport in Porous Media **70**, 213 (2007).

[14] A. Lenci, F. Zeighami, and V. Di Federico, Transport in Porous Media **144**, 459 (2022).

[15] M. Sahimi, *Heterogeneous Materials I: Linear transport and optical properties* (Springer Science & Business Media, 2003).

[16] M. Fourar, R. Lenormand, M. Karimi-Fard, and R. Horne, Transport in Porous Media **60**, 353 (2005).

[17] C. Mei and J.-L. Auriault, Journal of Fluid Mechanics **222**, 647 (1991).

[18] M. Firdaouss, J.-L. Guermond, and P. Le Quéré, Journal of Fluid Mechanics **343**, 331 (1997).

[19] X. Wang, F. Thauvin, and K. Mohanty, Chemical Engineering Science **54**, 1859 (1999).

[20] G. Firmani, A. Fiori, I. Jankovic, and G. Dagan, Multiscale Modeling & Simulation **7**, 1979 (2009).

[21] S. Kanaun and V. Levin, *Self-Consistent Methods for Composites: Static Problems* (Springer Science & Business Media, 2007).

[22] A. Fiori, I. Janković, and G. Dagan, Physical Review Letters **94**, 224502 (2005).

[23] G. Dagan, Water Resources Research **15**, 47 (1979).

[24] B. Abramovich and P. Indelman, Journal of Physics A: Mathematical and General **28**, 693 (1995).

[25] Z. Hashin and S. Shtrikman, Journal of Applied Physics **33**, 3125 (1962).

[26] S. Jones, in *SPE Annual Technical Conference and Exhibition* (OnePetro, 1987).

[27] D. Li and T. W. Engler, in *SPE permian basin oil and gas recovery conference* (OnePetro, 2001).

[28] M. G. Sidiropoulou, K. N. Moutsopoulos, and V. A. Tsihrintzis, Hydrological Processes **21**, 534 (2007).

[29] V. Di Federico, M. Pinelli, and R. Ugarelli, Stochastic Environmental Research and Risk Assessment **24**, 1067 (2010).

[30] G. Severino and A. Coppola, Transport in Porous Media **91**, 733 (2012).